Journal of Alloys and Compounds 527 (2012) 184–187

Contents lists available at SciVerse ScienceDirect

Journal of Alloys and Compounds

journal homepage: www.elsevier.com/locate/jallcom

In situ formation of superhard Cu–B based composite by reducing reaction

Wu Yuying*, Li Chong, Liu Xiangfa, Lu Kai

Key Laboratory for Liquid-Solid Structural Evolution and Processing of Materials, Ministry of Education, Shandong University, Ji'nan 250061, PR China

ARTICLE INFO

Article history:
Received 13 January 2012
Received in revised form 23 February 2012
Accepted 25 February 2012
Available online xxx

Keywords:
Electron microscopy
Non-ferrous alloys
Composite
Boron
Cu–B

ABSTRACT

In this work, superhard Cu–B based composite has been prepared by reducing reaction of B_2O_3 with Cu–Al melt. Moreover, the microstructure, microhardness, resistivity and CTE of Cu–B based composites has been studied. It has been found that B-rich compounds can be formed by reducing reaction occurred in the Cu–Al melt: $[Al] + B_2O_3 \rightarrow [B] + Al_2O_3$. The precipitation of B-rich compound may change the preferential growth plane of Cu matrix in Cu–B based composite. The average microhardness of the B-rich compound in Cu–10B alloy is 2763 HV, which is much higher than that of pure Cu. Moreover, CTE of Cu–10B alloy is much smaller than that of pure Cu, and the Cu–B composite has pretty good resistivity.

1. Introduction

The need for materials with high thermal conductivity and low coefficient of thermal expansion (CTE) is increasing as laser diodes and central processing units continue to require ever more special physical and mechanical properties. Since Cu metal matrix materials are expected to have special physical and mechanical properties, studies on the synthesis and characterization of Cu metal matrix composites have attracted increasing interest. Al_2O_3 [1–4], ZrO_2 [5], $MoSi_2$ [6], SiC [7–9] particles reinforced Cu metal matrix composites synthesized by different methods have been investigated for their excellent properties. In addition, diamond and boride ceramics possess many desirable properties, such as high hardness, high melting temperature, high modulus and high corrosion resistance [10–13], and these make them to be potential reinforcement candidates in copper matrix composites.

Although the properties of the Cu–diamond composites are excellent, the synthesis methods are mainly sintered, so they are relatively low thermal stability. The hardness of boron is very high, and it is also suitable for reinforcing the Cu matrix. However, pure B are always used during the preparation of Cu–B based composites [12,13], and it makes the preparation cost highly.

In the present work, B_2O_3 is used to prepare Cu–B based composites, and the Cu–B based composites are prepared by reducing reaction of B_2O_3 with Cu–Al melt. In addition, the microstructures, microhardness, resistivity and CTE of Cu–B based composites will be studied.

2. Experimental

The experimental materials used in this study were pure Cu (>99%, all compositions quoted in this work are in wt.% unless otherwise stated), pure Al (>99.99%), pure Si (>99%) and blocky B_2O_3. The preparation of Cu–B based composites was carried out according to the following procedure: (a) Pure Cu and pure Al (weight ratio 5% and 10%) for each test, weighting approximately 300 g were melted in an Al_2O_3 crucible using high-frequency induction furnace at about 1300 °C. (b) Then 1% pure Si and blocky B_2O_3 were added into the Cu–Al melt (the atomic ratio of B_2O_3 and Al was 1:2), stirred by graphite bar for 15 min. (c) The melt was poured into a steel mould, and cooled in the air.

Metallographic samples were mechanically ground and polished through standard routines. The microstructures of Cu–B based composites were observed and analyzed by SU-70 Scanning Electron Microscope (SEM). Phase identification was performed using X-ray diffraction. Microhardness was analyzed by HVS-1000 Digital Microhardness Tester, and the load was 50 g. Resistivity was measured using double-configuration four-point probe by H2ERM-1 resistance measuring device, and samples for resistivity test were machined with a size of $\Phi 8.5 \times 33\ mm^3$. CTE of Cu–B composites were investigated by a Netzsch DSC 404 calorimeter using pure In and Zn standards, and the detailed measurement processes to obtain the specific heat capacity were given by Bush and Johnson [14].

3. Results and discussion

3.1. Microstructures of Cu–B based composites

Microstructures of Cu–B based composites are observed by SU-70 SEM, as shown in Fig. 1. It can be found that a large number of reinforcing compounds distribute in the Cu matrix, and the amount of compounds increases with increasing addition level of Al and B_2O_3. More details of Cu–10B based composites are analyzed by

* Corresponding author. Tel.: +86 531 88392006; fax: +86 531 88395414.
E-mail address: wuyuying@sdu.edu.cn (Y. Wu).

0925-8388/$ – see front matter © 2012 Elsevier B.V. All rights reserved.
doi:10.1016/j.jallcom.2012.02.168

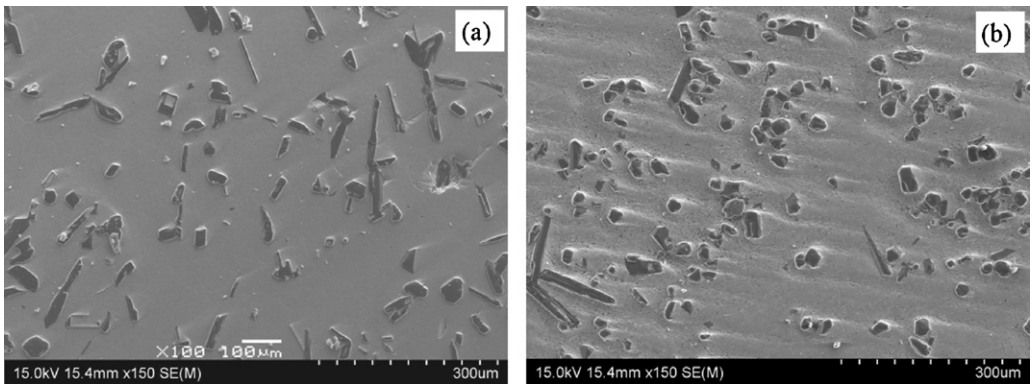

Fig. 1. Microstructures of Cu–B based composites (a) Cu–5B and (b) Cu–10B.

SU-70 SEM, as shown in Fig. 2. Fig. 2(b) shows the EDX of reinforcing B-rich compounds. The EDX result reveals that elements B, Al and Cu constitute the precipitated particles, with element atomic proportion B 94.32%, Al 3.01% and Cu 2.67%. Fig. 2(d) shows the EDX of matrix of Cu–10B based composites. It can be found that besides Cu, a small quantity of elements Al, Si and O can also be found in the Cu matrix. So it can be deduced that reducing reaction occurred in the Cu–Al melt:

$$[Al] + B_2O_3 \rightarrow [B] + Al_2O_3$$

Since the proportion of B in the B-rich compound is particularly high, it can be deduced that most of Al has been reacted with B_2O_3 in the Cu melt. Moreover, small amount of Al and Si are solutionizing in the Cu matrix.

3.2. XRD analysis of Cu–B based composites

More details of the obtained Cu–10B composite alloy are analyzed by XRD. Fig. 3 shows the XRD analysis of the Cu–10B based composite, and the XRD result reveals that the main components of the obtained composite are Cu and B-rich compounds as expected. Moreover, special attention has been paid to the parameters of XRD results. Table 1 shows the crystal lattice parameters of Cu matrix in Cu–10B composite alloy. It can be seen from Table 1 that the interplanar spacing in this work is a little larger than that of Davey's work [15], and the closed packed plane has been changed. In Davey's work [15], the closed packed plane of Cu is ⟨1 1 1⟩, while it has been changed to ⟨2 2 0⟩ in this work. It can be deduced that the solution in the Cu matrix makes the interplanar spacing larger, and the precipitation of B-rich compounds may change the preferential growth

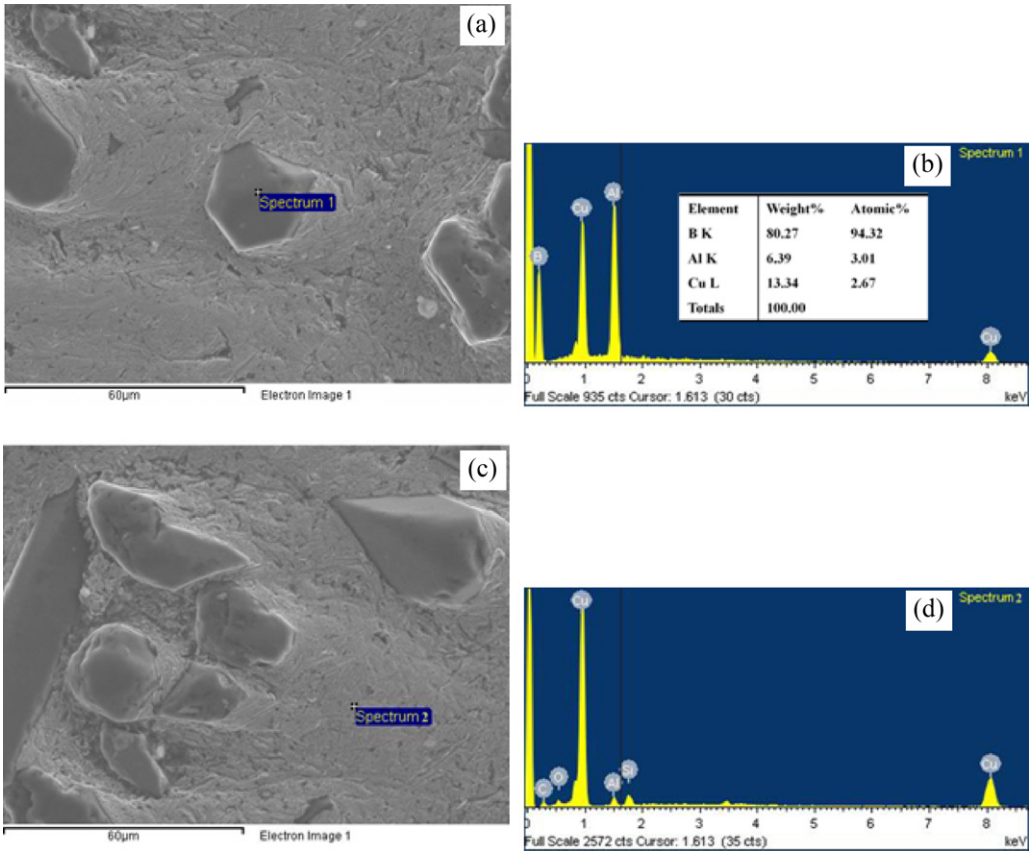

Fig. 2. SEM analysis of the phases in Cu–10B alloy (a) microstructure of Cu–10B alloy, (b) EDX analysis of dot 1, (c) microstructure of Cu–10B alloy, and (d) EDX analysis of dot 2.

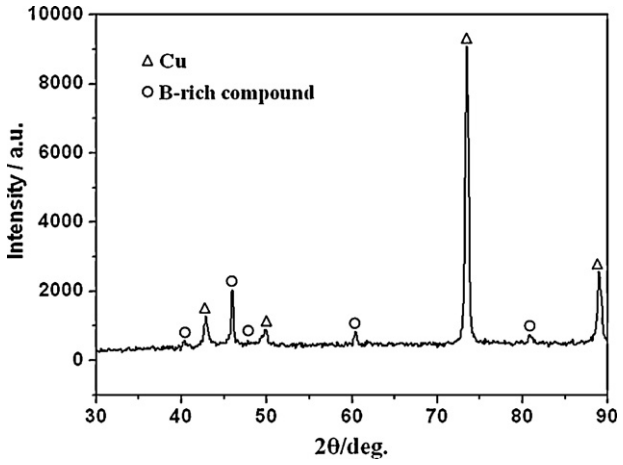

Fig. 3. XRD analysis of the Cu–10B based composite.

Table 1
Crystal lattice parameters of Cu in Cu–B based composite.

Peak list ($h\,k\,l$)	d in Ref. [15]	I in Ref. [15]	d in this work	I in this work
1 1 1	2.08	100	2.1054	15
2 0 0	1.80	86	1.8288	11
2 2 0	1.27	71	1.2880	100
3 1 1	1.09	86	1.0993	30

plane of Cu matrix in Cu–B based composite in this work. However, the exact influence mechanism needs to be further studied. Furthermore, the XRD peaks of B-rich compounds in this work are different from pure B, pure Al and AlB_2, and it has its own crystal structure and crystal parameters.

Fig. 4 shows the XRD analysis of the dross during preparation of Cu–10B based composite. Al_2O_3 and B_2O_3 can be found in the dross during preparation of Cu–10B based composite. So it can be confirmed that reducing reaction has occurred in the Cu–Al melt:

$$[Al] + B_2O_3 \rightarrow [B] + Al_2O_3$$

The density of Al_2O_3 is lower than that of Cu, so most Al_2O_3 floats on the surface of the Cu melt. When the melt was poured into the mould, most Al_2O_3 transformed into dross, and it cannot be found in the microstructure of Cu–B alloy. The B_2O_3 in the dross is what has not been reacted.

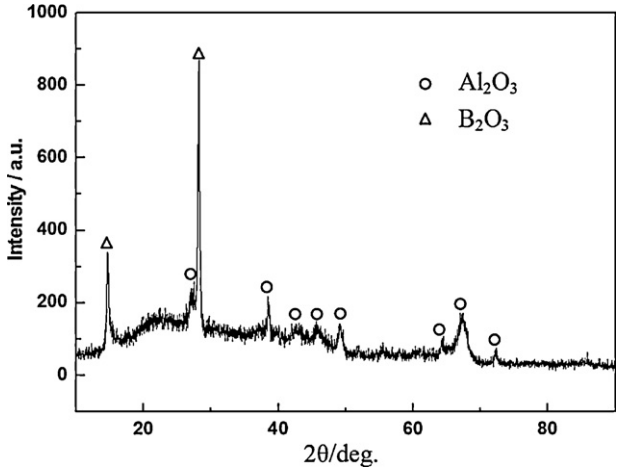

Fig. 4. XRD analysis of the dross during preparation of Cu–10B based composite.

Table 2
Microhardness and resistivity of Cu–10B based composite.

	Average microhardness (HV)		Resistivity (Ω m)
	B-rich compound	Cu matrix	
Cu–10B	2763	695.6	8×10^{-7}

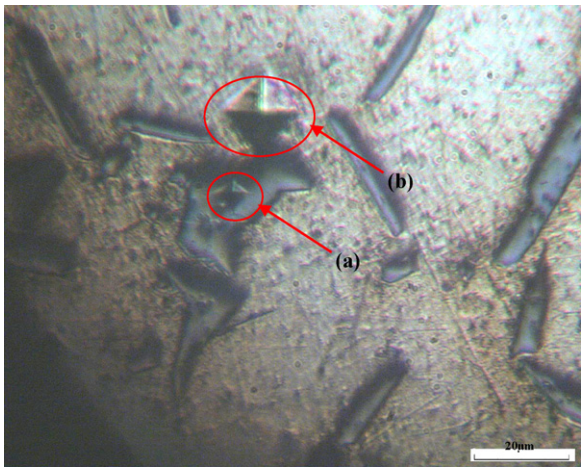

Fig. 5. Optical microscope image with indent on the B-rich compound and Cu matrix (a) indent on the B-rich compound and (b) indent on the Cu matrix.

3.3. The microhardness, resistivity and CTE of Cu–B based composite

Microhardness of pure Cu, the B-rich compound and Cu matrix in Cu–10B based composite has been measured by HVS-1000 Digital Microhardness Tester, as shown in Table 2, and the optical microscope image with indent on the B-rich compound and Cu matrix is shown in Fig. 5. The microhardness of the B-rich compound in Fig. 5 is 2806 HV. The microhardness of the pure Cu is 123 HV, but the microhardness of the Cu matrix solutionized by Al, Si and O in Cu–10B alloy can reach 695.6 HV, which has been improved by 465.5%. Moreover, the max microhardness of the B-rich compound in Cu–10B alloy can reach 2973 HV, and the average microhardness of the B-rich compound in Cu–10B alloy is 2763 HV. So it can be seen that the hardness of the Cu–10B composite has been improved significantly as compared to those of pure Cu.

The resistivity of Cu–10B composite have been tested using double-configuration four-point probe by H2ERM-1 resistance measuring device at 20 °C, and the resistivity has been calculated according to $\rho = RA/L$, where ρ is resistivity, R is electric resistance, A is cross-sectional area and L is the length of sample. As shown in

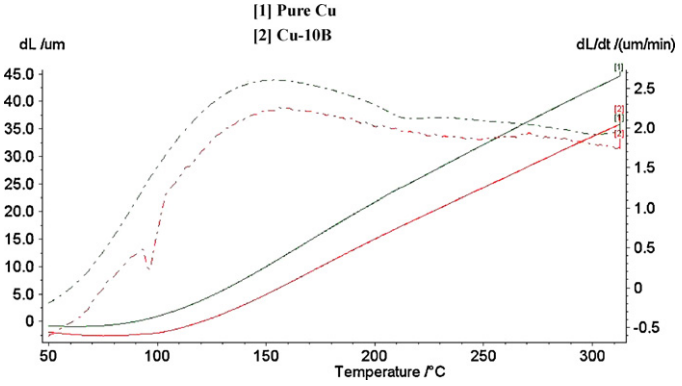

Fig. 6. CTE analysis of pure Cu and Cu–10B alloy.

Table 2, the resistivity of Cu–10B composite is $8 \times 10^{-7}\ \Omega$ m, which is a little higher than pure Cu at 20 °C. So the Cu–B composite has pretty good resistivity.

In addition, the CTE of pure Cu and Cu–10B has been measured in this work, as shown in Fig. 6. It can be seen that the CTE of Cu–10B alloy is much smaller than that of pure Cu. The maximum CTE of pure Cu is 2.6×10^{-6} at about 152 °C, while the maximum CTE of Cu–10B alloy is 2.25×10^{-6} at about 157 °C, which is much lower than that of pure Cu. Based on above discuss and results, it can be seen that the Cu–B based composites have higher hardness, lower CTE and pretty good resistivity, compared to pure Cu.

4. Conclusion

In this work, Cu–B based composites have been prepared by reducing reaction of B_2O_3 with Cu–Al melt, and B-rich compounds can be formed by reducing reaction occurred in the Cu–Al melt: $[Al] + B_2O_3 \rightarrow [B] + Al_2O_3$. The solution in the Cu matrix makes the interplanar spacing larger, and the precipitation of B-rich compounds changes the preferential growth plane of Cu matrix in Cu–B based composite. The average microhardness of the B-rich compound in Cu–10B alloy is 2763 HV, and the hardness of the Cu–10B composite has been improved significantly as compared to those of pure Cu. Moreover, CTE of Cu–10B alloy is much smaller than that of pure Cu, and the Cu–B composite has pretty good resistivity.

Acknowledgments

The authors wish to thank the support of National Natural Science Foundation of China under Projects 51001065, Shandong Province Natural Science Foundation (ZR2010EQ013) in China, Shandong Province Foundation for Outstanding Youth Scientist (BS2009CL035), Independent Innovation Foundation of Shandong University (2010TS081) and Postdoctoral Independent Innovation Foundation of Shandong Province (200901009).

References

[1] M.S. Motta, P.K. Jena, E.A. Brocchi, I.G. Solorzano, Mater. Sci. Eng. C 15 (2001) 175–177.
[2] P.K. Jena, E.A. Brocchi, M.S. Motta, Mater. Sci. Eng. A 313 (2001) 180–186.
[3] D.W. Lee, B.K. Kim, Mater. Lett. 58 (2004) 378–383.
[4] D.Y. Ying, D.L. Zhang, Mater. Sci. Eng. A 286 (2000) 152–156.
[5] J. Ding, N.Q. Zhao, C.S. Shi, X.W. Du, J.J. Li, J. Alloys Compd. 425 (2006) 390–394.
[6] Q.D. Hu, P. Luo, D. Qiao, Y.W. Yan, J. Alloys Compd. 464 (2008) 157–161.
[7] H.K. Kang, S.B. Kang, Mater. Sci. Eng. A 428 (2006) 336–345.
[8] R. Zhang, L. Gao, J.K. Guo, Composites Part A 35 (2004) 1301–1305.
[9] K.E. Pappacena, M.T. Johnson, S. Xie, K.T. Faber, Compos. Sci. Technol. 70 (2010) 485–491.
[10] Y. Wang, Q.C. Jiang, Y.Q. Zhao, F. Zhao, F. Zhao, B.X. Ma, Y. Wang, Mater. Sci. Eng. A 372 (2004) 109–114.
[11] K.A. Weidenmann, R. Tavangar, L. Weber, Mater. Sci. Eng. A 523 (2009) 226–234.
[12] L. Weber, R. Tavangar, Scr. Mater. 57 (2007) 988–991.
[13] D.B. Liu, M.F. Chen, A. Rauf, C.X. Cui, J.J. Tan, J. Alloys Compd. 466 (2008) 87–91.
[14] R. Bush, W.L. Johnson, J. Appl. Phys. 83 (1998) 4134–4141.
[15] Wheeler P. Davey, Phys. Rev. 25 (1925) 753–761.